

The intermediate-age open clusters Ruprecht 4, Ruprecht 7 and Pismis 15

G. Carraro^{1,2} \star , D. Geisler³, G. Baume⁴, R. Vázquez⁴, and A. Moitinho⁵

¹*Departamento de Astronomía, Universidad de Chile, Casilla 36-D, Santiago, Chile*

²*Astronomy Department, Yale University, P.O. Box 208101, New Haven, CT 06520-8101, USA*

³*Universidad de Concepción, Departamento de Física, Casilla 160-C, Concepción, Chile*

⁴*Facultad de Ciencias Astronómicas y Geofísicas de la UNLP, IALP-CONICET, Paseo del Bosque s/n, La Plata, Argentina*

⁵*CAAUL, Observatório Astronómico de Lisboa, Tapada da Ajuda, 1349-018 Lisboa, Portugal*

Submitted: February 2005

ABSTRACT

We report on *BVI* CCD photometry to $V = 22.0$ for 3 fields centered on the region of the Galactic star clusters Ruprecht 4, Ruprecht 7 and Pismis 15 and on 3 displaced control fields. Ruprecht 4 and Pismis 15 have never been studied before, and we provide for the first time estimates of their fundamental parameters, namely, radial extent, age, distance and reddening. Ruprecht 7 (Berkeley 33) however was studied by Mazur et al. (1993). We find that the three clusters are all of intermediate age (0.8–1.3 Gyr), and with a metallicity close to or lower than solar.

Key words: Open clusters and associations: general – open clusters and associations: individual: Ruprecht 4, Ruprecht 7 and Pismis 15

1 INTRODUCTION

This paper belongs to a series dedicated to the study of the open clusters population in the third Galactic Quadrant, and aiming at addressing fundamental questions like the structure of the spiral arms in this quadrant, and the precise definition of the Galactic disk radial abundance gradient outside the solar circle. A more detailed illustration of the motivations of this project are given in Moitinho (2001) and Baume et al (2004). Here we concentrate on three intermediate-age clusters (about the age of the Hyades - 600 Myrs - or older), Ruprecht 4, Ruprecht 7 and Pismis 15, for which we provide new photometric data and try to clarify their nature and to derive the first estimates of their fundamental parameters. The layout of the paper is as follows. Sect. 2 illustrates the observation and reduction strategies. An analysis of the geometrical structure and star counts in the field of the clusters are presented in Sect. 3, whereas a discussion of the Color-Magnitude Diagrams (CMD) is performed in Sect. 4. Sect. 5 deals with the determination of clusters reddening, distance and age and, finally, Sect. 6 summarizes our findings.

Table 1. Basic parameters of the clusters under investigation. Coordinates are for J2000.0 equinox

Name	<i>RA</i>	<i>DEC</i>	<i>l</i>	<i>b</i>
	<i>hh : mm : ss</i>	<i>° : ' : ''</i>	[deg]	[deg]
Ruprecht 4	06:48:59	-10:31:10	222.04	-5.31
Ruprecht 7	06:57:52	-13:13:25	225.44	-4.58
Pismis 15	09:34:45	-48:02:19	272.49	+2.86

2 OBSERVATIONS AND DATA REDUCTION

CCD *BVI* observations were carried out with the CCD camera on-board the 1.0m telescope at Cerro Tololo Inter-American Observatory (CTIO, Chile), on the nights of December 13 and 15, 2004. With a pixel size of $0''.469$, and a CCD size of 512×512 pixels, this samples a $4'.1 \times 4'.1$ field on the sky.

The details of the observations are listed in Table 2 where the observed fields are reported together with the exposure times, the average seeing values and the range of air-masses during the observations. Figs. 1 to 3 show finding charts in the area of Ruprecht 4, Ruprecht 7 and Pismis 15, respectively.

\star On leave from Dipartimento di Astronomia, Università di Padova, Vicolo Osservatorio 2, I-35122, Padova, Italy. email: gcar-raro@das.uchile.cl

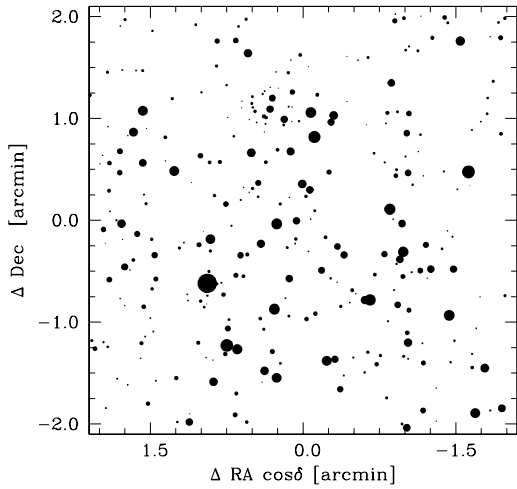


Figure 1. *V* Finding charts in the region of the open cluster Ruprecht 4. The size of the dots are proportional to the star magnitude. North is up, east on the left, and the covered area is $4'.1 \times 4'.1$

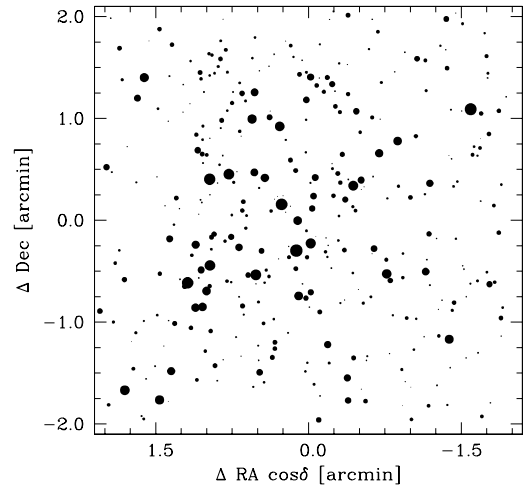


Figure 2. *V* Finding chart in the region of the open cluster Ruprecht 7. The size of the dots are proportional to the star magnitude. North is up, East on the left, and the covered area is $4'.1 \times 4'.1$

The data have been reduced with the IRAF[†] packages CCDRED, DAOPHOT, ALLSTAR and PHOTCAL using the point spread function (PSF) method (Stetson 1987). The two nights turned out to be photometric and very stable, and therefore we derived calibration equations for all the 130 standard stars observed during the two nights in the Landolt (1992) fields SA 95-41, PG 0231+051, Rubin 149, Rubin 152, T phe and SA 98-670 (see Table 2 for details). Together with the clusters, we observed three control fields 20 arcmins apart from the nominal cluster centers to deal with field star contamination. Exposure of 600 secs in *V* and *I* were secured for these fields.

The calibration equations turned out to be of the form:

$$\begin{aligned} b &= B + b_1 + b_2 * X + b_3 (B - V) \\ v &= V + v_1 + v_2 * X + v_3 (B - V) \\ v &= V + v_{1,i} + v_{2,i} * X + v_{3,i} * (V - I) \\ i &= I + i_1 + i_2 * X + i_3 (V - I) , \end{aligned}$$

where *BVI* are standard magnitudes, *bvi* are the instrumental ones and *X* is the airmass; all the coefficient values are reported in Table 3. The standard stars in these fields provide a very good color coverage. The final *r.m.s.* of the calibration are 0.039, 0.034 and 0.033 for the *B*, *V* and *I* filters, respectively.

We generally used the third equation to calibrate the *V* magnitude in order to get the same magnitude depth both in the cluster and in the field. Photometric errors have been estimated following Patat & Carraro (2001). It turns out that stars brighter than $V \approx 22$ mag have internal (ALLSTAR

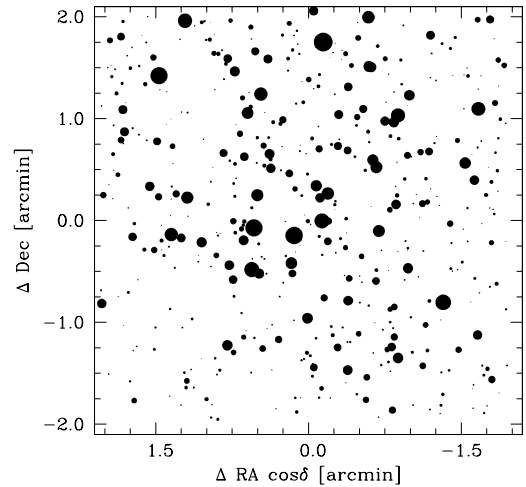


Figure 3. *V* Finding chart in the region of the open cluster Pismis 15. The size of the dots are proportional to the star magnitude. North is up, East on the left, and the covered area is $4'.1 \times 4'.1$

output) photometric errors lower than 0.10 mag in magnitude and lower than 0.18 mag in color, as one can readily see by inspecting Fig. 3. There the trend of errors in colors and magnitude are reported against the *V* mag.

The final photometric catalog for Ruprecht 4, Ruprecht 7 and Pismis 15 (coordinates, *B*, *V* and *I* magnitudes and er-

[†] IRAF is distributed by NOAO, which are operated by AURA under cooperative agreement with the NSF.

Table 2. Journal of observations of Ruprecht 4, Ruprecht 7 and Pismis 15 and standard star fields (December 13 and 15, 2004).

Field	Filter	Exposure time [sec.]	Seeing [\prime]	Airmass
Ruprecht 4	B	120,1200	1.2	1.12-1.20
	V	30,600	1.3	1.12-1.20
	I	30,600	1.2	1.12-1.20
Ruprecht 7	B	120,1200	1.2	1.12-1.20
	V	30,600	1.3	1.12-1.20
	I	30,600	1.2	1.12-1.20
Pismis 15	B	120,1200	1.2	1.12-1.20
	V	30,600	1.3	1.12-1.20
	I	30,600	1.2	1.12-1.20
SA 98-671	B	3×120	1.2	1.24-1.26
	V	3×40	1.4	1.24-1.26
	I	3×20	1.4	1.24-1.26
PG 0231+051	B	3×120	1.2	1.20-2.04
	V	3×40	1.5	1.20-2.04
	I	3×20	1.5	1.20-2.04
T Phe	B	3×120	1.2	1.04-1.34
	V	3×40	1.3	1.04-1.34
	I	3×20	1.3	1.04-1.34
Rubin 152	B	3×120	1.3	1.33-1.80
	V	3×40	1.2	1.33-1.80
	I	3×20	1.2	1.33-1.80
Rubin 149	B	3×120	1.1	1.21-1.96
	V	3×40	1.2	1.21-1.96
	I	3×20	1.2	1.21-1.96
SA 95-41	B	3×120	1.2	1.05-1.48
	V	3×40	1.2	1.05-1.48
	I	3×20	1.1	1.05-1.48

Table 3. Coefficients of the calibration equations

$b_1 = 3.465 \pm 0.009$	$b_2 = 0.25 \pm 0.02$	$b_3 = -0.145 \pm 0.008$
$v_1 = 3.244 \pm 0.005$	$v_2 = 0.16 \pm 0.02$	$v_3 = 0.021 \pm 0.005$
$i_1 = 4.097 \pm 0.005$	$i_2 = 0.08 \pm 0.02$	$i_3 = 0.006 \pm 0.005$
$i_1 = 4.097 \pm 0.005$	$i_2 = 0.08 \pm 0.02$	$i_3 = 0.006 \pm 0.005$

rors) consists of 953, 769 and 1007 stars, respectively, and are made available in electronic form at the WEBDA[‡] site maintained by J.-C. Mermilliod.

3 STAR COUNTS AND CLUSTER SIZE

Since our photometry covers entirely each cluster's area we performed star counts to obtain an improved estimate of the clusters size. We derived the surface stellar density by performing star counts in concentric rings around the clusters nominal centers (see Table 1) and then dividing by their respective area. Poisson errors have also been derived and

[‡] <http://obswww.unige.ch/webda/navigation.html>

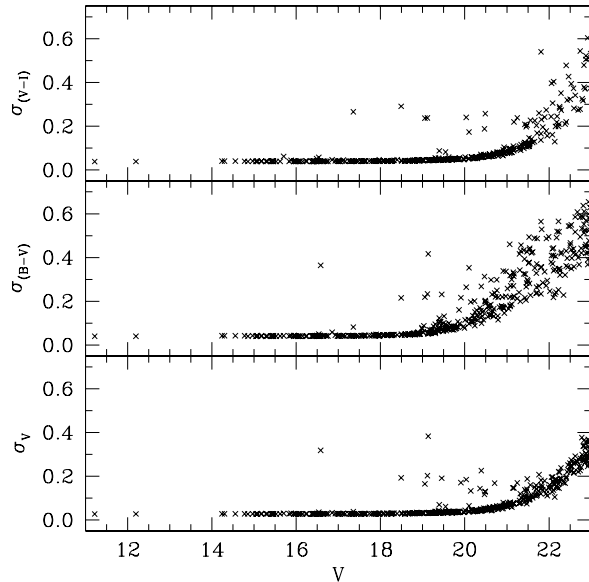


Figure 4. Trend of photometric errors in V , $(B-V)$ and $(V-I)$ as a function of V magnitude.

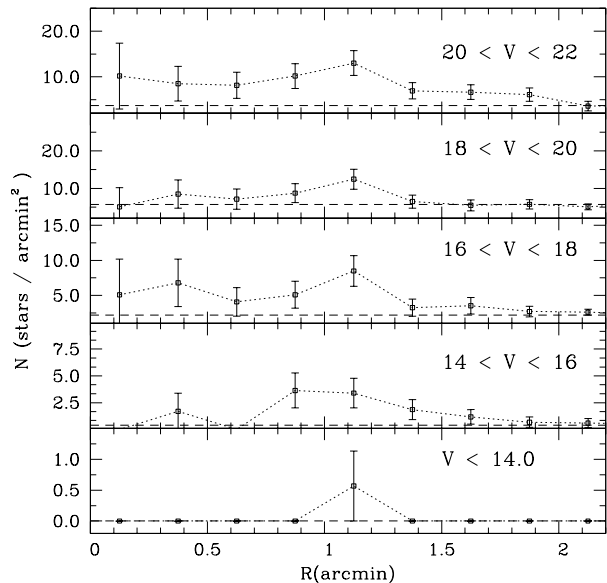


Figure 5. Star counts in the area of Ruprecht 4 as a function of radius and magnitude. The dashed lines represent the level of the control field counts estimated in the surroundings of the cluster in that magnitude range.

normalized to the corresponding area. The field star contribution has been derived from the control field which we secured for each cluster.

Ruprecht 4 The final radial density profile for Ruprecht 4 is shown in Fig. 5 as a function of V magnitude. Clearly, the cluster does not appear concentrated, and at the nominal cluster center we can see a deficiency of stars, which on the are hand populated a sort a ring-like structure

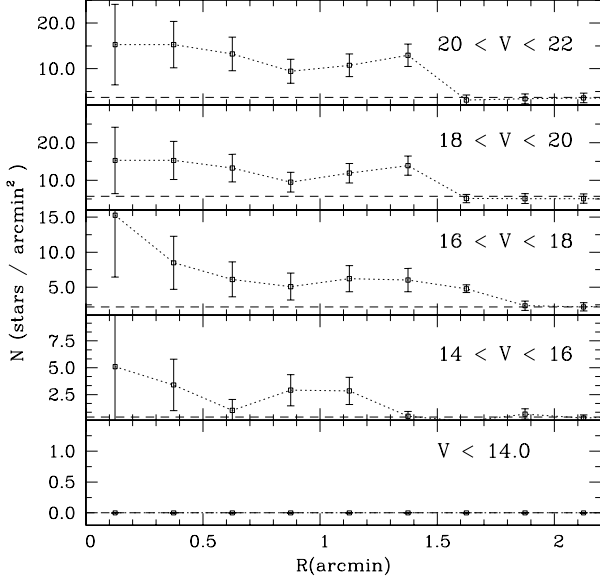


Figure 6. Star counts in the area of Ruprecht 7 as a function of radius and magnitude. The dashed lines represent the level of the control field counts estimated in the surroundings of the cluster in that magnitude range.

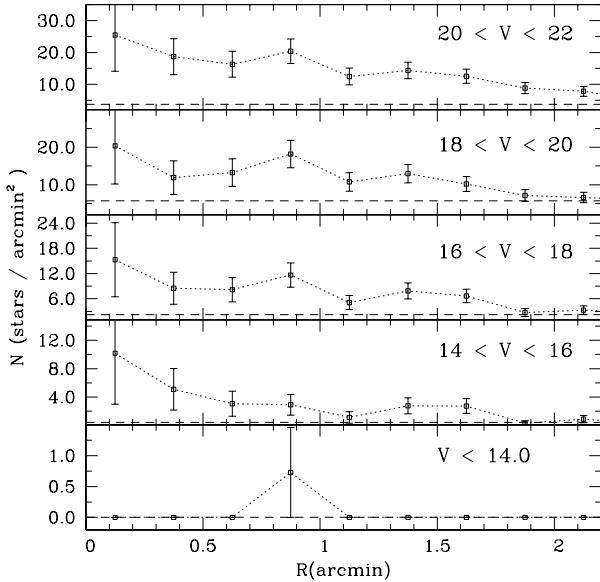


Figure 7. Star counts in the area of Pismis 15 as a function of radius and magnitude. The dashed lines represent the level of the control field counts estimated in the surroundings of the cluster in that magnitude range.

(see also Fig. 1) at 1.5 arcmin from the center. This is not unusual for open clusters, which in many cases are sparse objects.

The cluster seems to be populated by stars of magnitude in the range $15 \leq V \leq 22$, where it clearly emerges from the background. In this magnitude range the radius is not larger

than 1.5 arcmin. We shall adopt the value of 1.5 arcmin as the Ruprecht 4 radius throughout this paper. This estimate is smaller than the value of 4.5 arcmin reported by Dias et al. (2002) for the cluster diameter.

Ruprecht 7 The final radial density profile for Ruprecht 7 is shown in Fig. 6 as a function of V magnitude. The cluster seems to be populated by stars of magnitude in the range $14 \leq V \leq 22$, where it clearly emerges from the background. In this magnitude range the radius is not larger than 1.5 arcmin. In conclusion, we are going to adopt the value of 1.5 arcmin as the Ruprecht 7 radius throughout this paper. This estimate is smaller than the value of 4.0 arcmin reported by Dias et al. (2002) for the cluster diameter.

Pismis 15 The final radial density profile for Pismis 15 is shown in Fig. 7 as a function of V magnitude. The cluster seems to be populated by stars of magnitude in the range $14 \leq V \leq 22$, where it clearly emerges from the background. In this magnitude range the radius is not larger than 1.8 arcmin. In conclusion, we are going to adopt the value of 1.8 arcmin as the Pismis 15 radius throughout this paper. This estimate is in good agreement with the value of 4.0 arcmin reported by Dias et al. (2002) for the cluster diameter.

The estimates we provide for the radius, although reasonable, must be taken as preliminary. In fact the size of the CCD is probably too small to derive conclusive estimates of the cluster sizes. This is particularly true in the case Pismis 15, for which the cluster radius we derived must be considered as a lower limit of the real cluster radius. In fact, while for Ruprecht 4 and 7 the cluster density profile converges toward the field level within the region covered by the CCD, in the case of Pismis 15 the cluster dominates the star counts - at least for the faintest stars - up to the border of the region we covered. Larger field coverage is necessary in this case to derive a firm estimate of the cluster radius.

4 THE COLOUR-MAGNITUDE DIAGRAMS

In Fig. 8 we present the CMDs we obtained for the three clusters under investigation. In this figure the open cluster Ruprecht 4 is shown together with the corresponding control field in the lower panels, whereas Ruprecht 7 and Pismis 15 are presented in the middle and upper panels, respectively. The control fields help us to better interpret these CMDs, which are clearly dominated by foreground star contamination.

Ruprecht 4. This cluster is presented in the lower panels of Fig. 8. It exhibits a Main Sequence (MS) extending from $V=16$, where the Turn Off Point (TO) is located down to $V=22$. This MS is significantly wide, a fact that we ascribe to the increasing photometric error at increasing magnitude, the field star contamination, and to the presence of a sizeable binary star population, which mainly enlarge the MS toward red colors. In particular the effect of a significant binary population is known to affect the MS and TO shape, which appear at first glance confused (see for comparison the CMDs in the middle and upper panels; for a reference see also Meynet et al. 1993).

However, the reality of this cluster seems to be secured by the shape of the MS with respect to the control field MS, which population sharply decrease at $V = 18$. Besides,

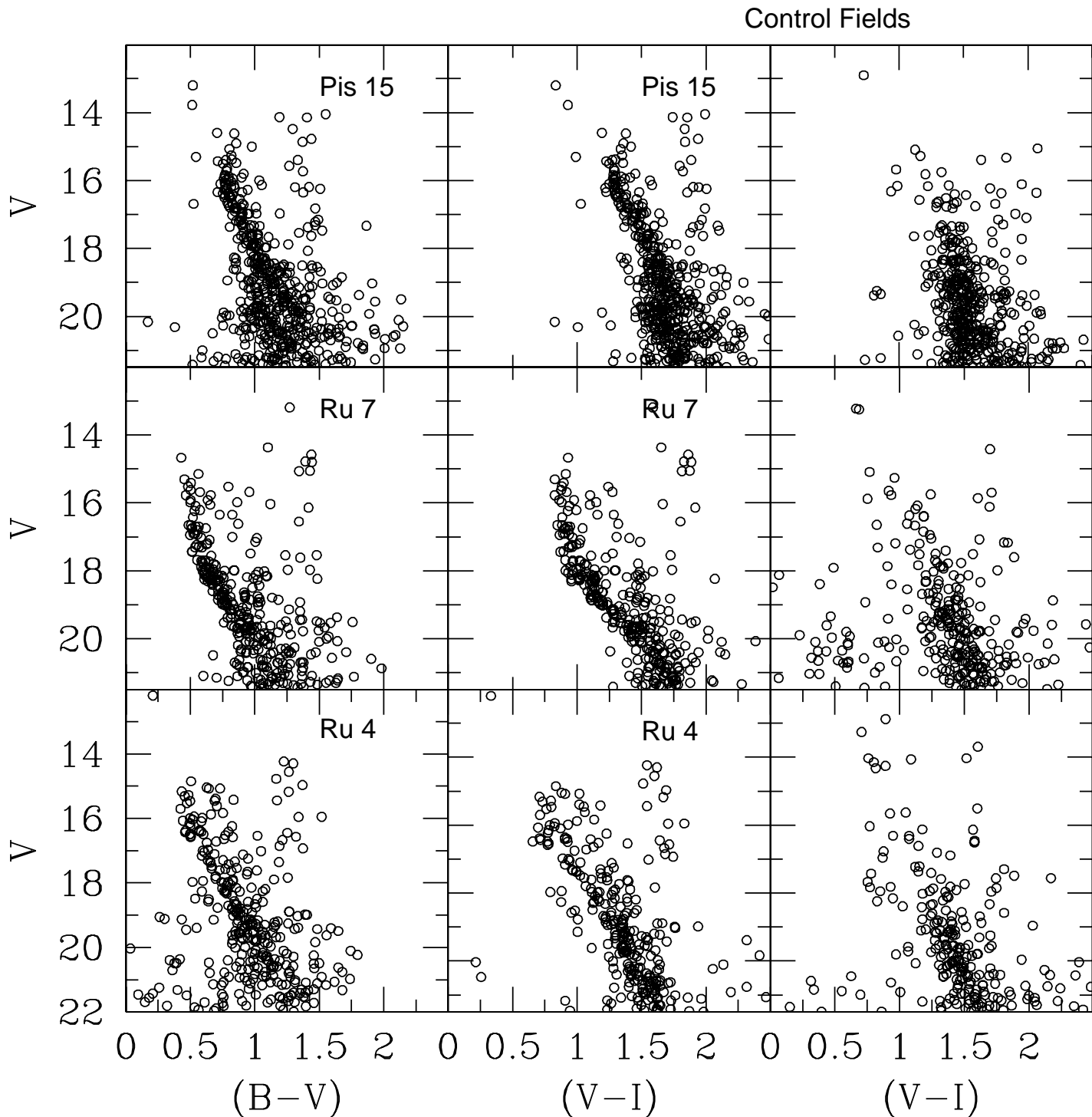


Figure 8. V vs $(B-V)$ (left panels) and V vs $(V-I)$ (middle panels) CMDs of Ruprecht 4 (lower panels), Ruprecht 15 (middle panels) and Pismis 15 (upper panels) and corresponding control fields (right panels). We include all stars in each field.

the cluster MS is significantly bluer and more tilted than the field MS, which derives from the superposition of stars of different reddening located at all distances between the cluster and the Sun. Another interesting evidence is the possible presence of a clump of stars at $V=15$, which does not

have a clear counterpart in the field, and which makes the cluster an intermediate-age one. In fact if we use the age calibration from Carraro & Chiosi (2004), for a ΔV (say the magnitude difference between the red clump and the TO) of 1 mag, we infer an age around 1 billion year. This esti-

mate does not take into account the cluster metallicity, and therefore is simply a guess. In the following we shall provide a more robust estimate of the age through a detailed comparison with theoretical isochrones.

Ruprecht 7. The open cluster Ruprecht 7 is presented in the middle panels of Fig. 8. The interpretation of this CMD seems much easier than the previous one. Here the MS is more evident, the TO is located at $V \approx 15.5$, and the clump at $V \approx 15$, thus implying a rough estimate for the age around 0.5 billion year. The overall morphology of the CMDs is so different from the field CMD that it leaves no doubt on the cluster reality. Also in this case the distribution of the stars in the red edge of the MS suggests a probably binary star population. Both Ruprecht 4 and Ruprecht 7 has a clump mean magnitude $V=15$. According to Salaris & Girardi (2002), this implies a common distance modulus (m-M) of about 15 mag.

Pismis 15. The open cluster Pismis 15 is finally presented in the upper panels of Fig. 8. The TO is located at $V \approx 16$, and the clump at $V \approx 14.5$, thus implying a rough estimate for the age around 1.5 billion year. The overall morphology of the CMDs is also in this case very different from the field CMD so this is a bona-fide cluster. A word of caution is mandatory because the precise clump position is affected by field star contamination in the form of a tail of stars which connects the clump with the MS at $V = 18$. Again, the control field helps us to interpret the CMD. Indeed also in the control field there is a vertical sequence detaching from the MS at $V=18$, which however stops at $V = 15$, supporting the interpretation of the 5-6 bright red stars as clump stars with mean $V = 14.5$. This suggests that Pismis 15 might be somewhat closer to the Sun than the two other clusters.

5 DERIVING CLUSTERS' FUNDAMENTAL PARAMETERS

In this section we are going to perform a detailed comparison of the star distribution in the clusters CMDs with theoretical isochrones. We adopt in this study the Padova library from Girardi et al. (2000). This comparison is clearly not an easy exercise. In fact the detailed shape and position of the various features in the CMD (MS, TO and clump basically) depends mostly on age and metallicity, and then also on reddening and distance. The complex interplay between the various parameters is well known, and we refer to Chiosi et al. (1992) and Carraro (2005) as nice examples of the underlying technique.

Our basic strategy is to survey different age and metallicity isochrones attempting to provide the best fit of all the CMD features both in the V vs $(B - V)$ and in the V vs $(V - I)$ CMD.

Besides, to further facilitate the fitting procedure we shall consider only the stars which lie within the cluster radius as derived in Sect. 3. Therefore, in the series of Figs. 9 to 11 we shall present the best fit we were able to achieve. Together with the best fit, we could make estimates of uncertainties in the basic parameters derivation. These uncertainties simply reflect the range in the basic parameter which allow a reasonable fit to the clusters CMDs. Error estimates are re-

ported in Table 4.

Finally, to derive clusters' distances from reddening and apparent distance modulus, a reddening law must be specified. In Fig. 9 we show that the normal extinction law is valid for all the clusters, and therefore we shall use the relation $A_v = 3.1 \times E(B - V)$ to derive clusters' distances. In details, the solid line in Fig. 9 is the normal extinction $E(V - I) = 1.245 \times E(B - V)$ law from Cousin (1978), whereas the dashed and dotted lines are the luminosity class *III* and *V* ZAMS, respectively.

Ruprecht 4. The isochrone solution for this cluster is discussed in Fig. 10. We obtained the best fit for an age of 800 million years and a metallicity $Z=0.008$, quite low for an open cluster of this age. The inferred reddening and apparent distance modulus are $E(B-V)=0.36$ ($E(V-I)=0.50$) and $(m-M)=14.6$, respectively. As a consequence the cluster possesses a heliocentric distance of 4.9 kpc, and is located at a Galactocentric distance of 12.0 kpc, assuming 8.5 kpc as the distance of the Sun to the Galactic Center. Interestingly, this cluster appears to be relatively young but very metal poor. This is not an isolated case, and Moitinho et al. (2005) reported on a similar case, the star cluster NGC 2635. The overall fit is very good, the detailed shape of the MS and TO are nicely reproduced, and the color of the clump as well.

Ruprecht 7 The isochrone solution for this cluster is discussed in Fig. 11. We obtained the best fit for an age of 800 million years and a metallicity $Z=0.019$. This metallicity is larger than the one proposed by Mazur et al. (1993), which was based on a comparison with isochrone from Bertelli et al. (1994). The inferred reddening and apparent distance modulus are $E(B-V)=0.30$ ($E(V-I)=0.47$) and $(m-M)=15.0$, respectively. As a consequence the cluster lies at 6.5 kpc from the Sun, and is located at a Galactocentric distance of 13.8 kpc toward the anti center direction. The overall fit is very good also in this case, the detailed shape of the MS and TO are nicely reproduced, and the color of the clump as well.

With respect to Mazur et al. (1993) study, we obtain a larger distance. However, both the age and the reddening are compatible with that study. We believe that the larger distance is due to the different isochrones set and mostly to the higher metallicity here adopted for this cluster.

Pismis 15. The isochrone solution for this cluster is discussed in Fig.12. We obtained the best fit for an age of 1300 million year and a metallicity $Z=0.008$. The inferred reddening and apparent distance modulus are $E(B-V)=0.53$ ($E(V-I)=0.88$) and $(m-M)=14.0$, respectively. Therefore the cluster has a heliocentric distance of 2.9 kpc, and is located at a Galactocentric distance of 8.8 kpc. The overall fit is very good also in this case, the detailed shape of the MS and TO are nicely reproduced, and the color of the clump as well.

6 CONCLUSIONS

We have presented the first CCD *BVI* photometric study of the star clusters Ruprecht 4, Ruprecht 7 and Pismis 15. The CMDs we derive allow us to infer estimates of the clusters' basic parameters, which are summarized in Table 4. In detail, the fundamental findings of this paper are:

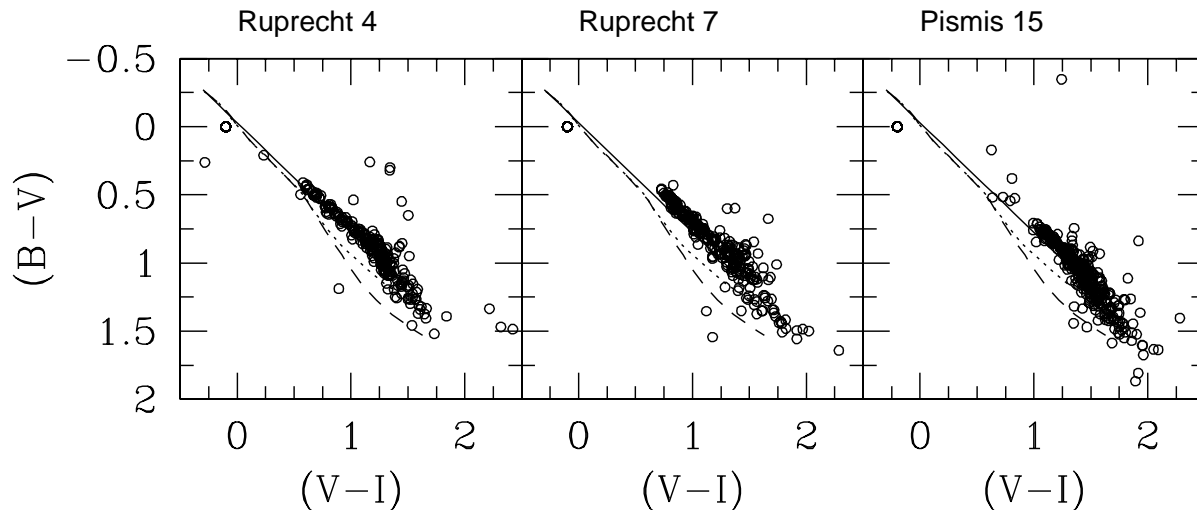


Figure 9. $B - V$ vs $V - I$ diagram for the three clusters. The solid line is the normal reddening law, whereas dashed and dotted lines are the luminosity class III and V ZAMS, respectively. See text for details.

Table 4. Fundamental parameters of the studied clusters. The coordinates system is such that the Y axis connects the Sun to the Galactic Center, while the X axis is perpendicular to that. Y is positive toward the Galactic anticenter, and X is positive in the first and second Galactic quadrants (Lynga 1982)

Name	Radius(arcmin)	$E(B - V)$	$E(V - I)$	$(m - M)$	d_{\odot}	$Y(kpc)$	$X(kpc)$	$Z(kpc)$	$R_{GC}(kpc)$	Age(Gyr)	Metallicity
Ruprecht 4	1.5	0.36 ± 0.1	0.50 ± 0.1	14.6 ± 0.2	4.9	-3.6	-3.3	-0.45	12.0	0.8 ± 0.2	0.008 ± 0.005
Ruprecht 7	1.5	0.30 ± 0.1	0.47 ± 0.1	15.0 ± 0.2	7.0	-4.6	-4.6	-0.50	13.8	0.8 ± 0.3	0.019 ± 0.002
Pismis 15	1.8	0.53 ± 0.1	0.88 ± 0.1	14.0 ± 0.2	2.9	0.1	-2.9	0.10	8.8	1.3 ± 0.3	0.008 ± 0.002

- the best fit reddening estimates support within the errors a normal extinction law toward the three clusters;
- Ruprecht 4 is an intermediate age open cluster whose position is compatible with the cluster belonging to the local spiral arm;
- Ruprecht 7 is a Hyades age cluster, although much poorer in metal than that cluster, and it is located at almost 14.0 kpc in the anti-center direction, thus being one of the most distant open cluster in the sense of the Galactocentric distance;
- Pismis 15 is an old open cluster located inside the solar ring, with a half than solar metal abundance. The distance we derived and its Galactic coordinates imply that the cluster probably belongs to the Carina spiral arm.

All these clusters are very interesting in the context of the chemical evolution of the Galactic disk (Geisler et al. 1992, Carraro et al. 1998, Friel et al 2002).

They may be very useful to trace the slope of the Galactic disk radial abundance gradient, which is very poorly sampled in the age range between 0.5 and 2 Gyr (see Friel et al 2002). If we make use of the provisional photometric estimates presented in this paper, we obtain that all the clusters basically confirm the most recent slope of the gradient as derive by Friel et al. (2002).

Further studies therefore should concentrate on the confirmation of the clusters' metal content by means of a detailed abundance analysis of the clump stars.

ACKNOWLEDGEMENTS

The observations presented in this paper have been carried out at Cerro Tololo Interamerican Observatory CTIO (Chile). CTIO is operated by the Association of Universities for Research in Astronomy, Inc. (AURA), under a cooperative agreement with the National Science Foundation as part of the National Optical Astronomy Observatory (NOAO). The work of G.C. is supported by *Fundación Andes*. D.G. gratefully acknowledges support from the Chilean *Centro de Astrofísica* FONDAF No. 15010003. This work has been also developed in the framework of the *Programa Científico-Tecnológico Argentino-Italiano SECYT-MAE Código: IT/PA03 - UIII/077 - período 2004-2005*. This study made use of Simbad and WEBDA databases.

REFERENCES

- Baume G., Moitinho A., Giorgi E., Carraro G., Vazquez R., 2004, *A&A* 417, 961
 Bertelli G., Bressan A., Chiosi C., Fagotto F., Nasi E., 1994 *A&AS* 106, 275

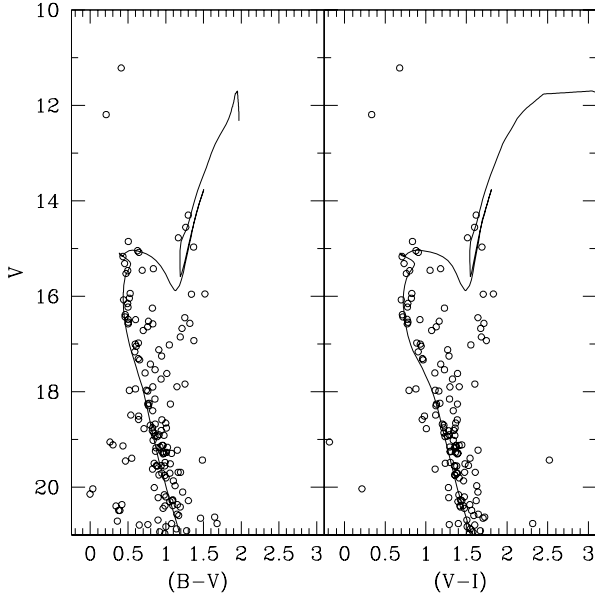


Figure 10. Isochrone solution for Ruprecht 4. The isochrone is for the age of 800 million year and metallicity $Z=0.008$. The apparent distance modulus is $(m-M)=14.6$, and the reddening $E(B-V)=0.36$ and $E(V-I)=0.50$. See text for more details. Only stars within the derived radius are shown.

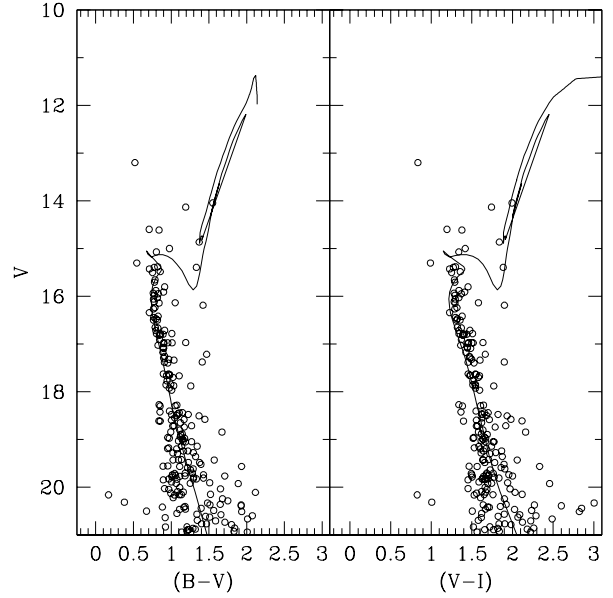


Figure 12. Isochrone solution for Pismis 15. The isochrone is for the age of 1300 million year and metallicity $Z=0.008$. The apparent distance modulus is $(m-M)=14.0$, and the reddening $E(B-V)=0.53$ and $E(V-I)=0.88$. See text for more details. Only stars within the derived radius are shown.

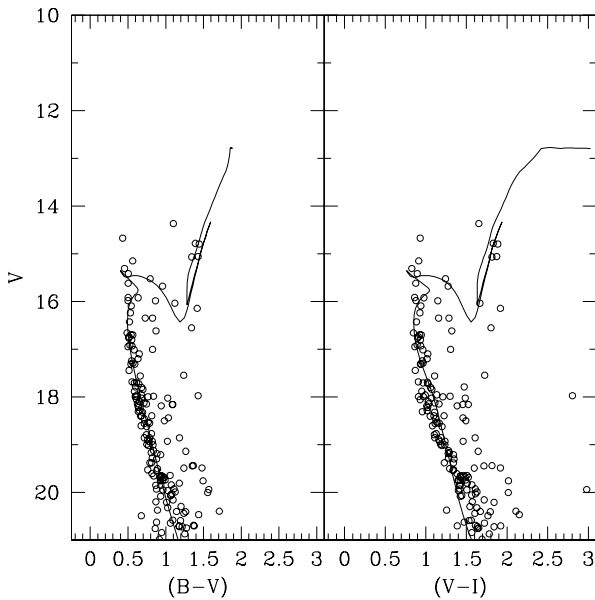


Figure 11. Isochrone solution for Ruprecht 7. The isochrone is for the age of 800 million year and metallicity $Z=0.019$. The apparent distance modulus is $(m-M)=15.0$, and the reddening $E(B-V)=0.30$ and $E(V-I)=0.47$. See text for more details. Only stars within the derived radius are shown.

- Carraro G., Chiosi C., 1994, *A&A* 287, 761
 Carraro G., Ng Y.K., Portinari L., 1998, *MNRAS* 296, 1045
 Carraro G., 2005, *ApJ* 621, L61
 Chiosi C., Bertelli G., Bressan A. 1992, *ARA&A* 30, 235
 Cousin A.W.J., 1978, *MNSSA* 37, 42
 Dias W.S., Alessi B.S., Moitinho A., Lepine J.R.D., 2002, *A&A* 389, 871
 Friel E.D., Janes K.A., Tavaroz M., Scott J., Katsanis R., Lotz J., Hong L. & Miller N. 2002, *AJ* 124, 2693
 Geisler D., Claria J.J., Minniti D., 1992, *AJ* 104, 1892
 Girardi L., Bressan A., Bertelli G., Chiosi C., 2000, *A&AS* 141, 371
 Landolt A.U., 1992, *AJ* 104, 340
 Lynga G., 1982, *A&A* 109, 213
 Mazur B., Kaluzny J., Krzeminski W., 1993, *MNRAS* 265, 405
 Meynet G., Mermilliod J-C. & Maeder A., 1993, *A&AS* 98, 477
 Moitinho A., 2001, *A&A* 370, 436
 Moitinho A., Carraro G., Baume G., Vazquez R., 2005, *A&A* submitted
 Patat F., Carraro G., 2001, *MNRAS* 325, 1591
 Salaris M., Girardi L., 2002, *MNRAS* 337, 332
 Schmidt-Kaler Th. 1982, *Landolt-Börnstein, Numerical data and Functional Relationships in Science and Technology, New Series, Group VI, Vol. 2(b)*, K. Schaifers and H.H. Voigt Eds., Springer Verlag, Berlin, p.14
 Stetson P.B. 1987, *PASP* 99, 191